J Solid State Electrochem (2012) 16:353–360
DOI 10.1007/s10008-011-1339-2

ORIGINAL PAPER

Electrochemical characterization and stress corrosion cracking behavior of α-brass in molybdate-containing electrolytes

Nageh K. Allam · Ahmed Abdel Nazeer · Elsayed A. Ashour

Received: 30 November 2010 / Revised: 5 February 2011 / Accepted: 8 February 2011 / Published online: 25 March 2011

Abstract One of the major challenges in material design is the achievement of reasonable operational efficiency through understanding the factors affecting the material's performance particularly strength and service lifetime characteristics. In this work, the electrochemical behavior of 72Cu–28Zn α-brass alloy in Na_2MoO_4-containing electrolytes was investigated using potentiodynamic polarization and electrochemical frequency modulation techniques complemented with scanning electron microscopy. Also, stress corrosion cracking behavior of the alloy under both open-circuit potential and anodic applied potentials, using the slow strain rate technique, was evaluated. The results drawn from the different techniques are comparable.

Keywords α-Brass · Stress corrosion cracking · Pitting · Molybdate · Frequency modulation

Introduction

Brasses, alloys of copper and zinc, are widely used in different intricate and critically important industries as condensers, heat exchanger tube materials, tubes in sugar juice evaporators and building plumbing systems, and distillation type desalination plants [1–3]. During operation, these parts are subject to different stresses beside the influence of some electrolytic solutions containing oxyanions which sometimes lead to failure of these parts by stress corrosion cracking (SCC) [4]. Kawashima et al. studied the SCC of admiralty brass in various oxyanions (NO_2^-, NO_3^-, ClO_3^-, SO_4^{2-}, WO_4^{2-}, CrO_4^{2-}, etc.) at a controlled potential of 300 mV [4, 5]. They found the severity of cracking to depend on the type and concentration of oxyanions present in the test solutions with the cracking always found to be transgranular with considerable branching in some cases. Allam et al. studied the effect of annealing on the SCC susceptibility of brass in some oxyanions (ClO_3^-, NO_2^-, and SO_4^{2-}) [6]. The annealed specimens were found to suffer from SCC in all tested electrolytes under anodic polarization conditions while they were susceptible to SCC only in NO_2^- and SO_4^{2-} solutions under the open-circuit condition. The susceptibility toward SCC was found to decrease considerably in ClO_3^- and SO_4^{2-} solutions and very slightly in NO_2^- solutions upon annealing the specimens. Although the SCC of brass was tested in a plethora of oxyanion-containing electrolytes [4–7], it seems that the electrochemical and SCC behavior of brass in molybdate-containing electrolytes is not fully investigated.

Given the multitude of factors that may influence brass performance in various electrolyte systems, it is clear that predicting the consequences is not an easy task. Fortunately, it may be possible to identify the predominant controlling factors to better assess the likelihood of SCC occurrence and consequences. As the selection of a

N. K. Allam (✉) · A. A. Nazeer · E. A. Ashour
Electrochemistry and Corrosion Laboratory,
Physical Chemistry Department, National Research Centre,
Cairo 12622, Egypt
e-mail: Nageh.Allam@gmail.com

specific brass alloy for a certain application is usually based on laboratory test results that were obtained in the simulated environment, the purpose of the present work was to study the electrochemical and SCC behavior of brass in solutions containing different concentrations of molybdate anions using potentiodynamic polarization and the electrochemical frequency modulation (EFM) techniques to identify some of the factors and conditions affecting its susceptibility towards SCC in such solutions and also to investigate the mode and mechanism of cracking.

Experimental

The material used was α-brass of the following chemical composition: 71.7% Cu, 28.284% Zn, 0.006% Pb, and 0.01% Fe. The mechanical properties are given as: ultimate tensile strength=283 N mm^{-2} (28.8 kg mm^{-2}), yield strength=216 N mm^{-2} (22.0 kg mm^{-2}), Vickers's hardness=600 N mm^{-2} (61.0 kg mm^{-2}), and elongation=80%. Measurements were performed at a constant strain rate of 1.5×10^{-5} s^{-1}. The tensile test specimens were designed to have the following dimensions:

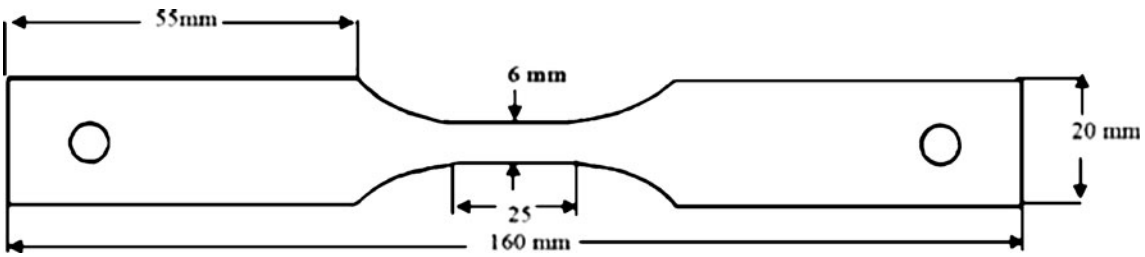

Before conducting the tests, the specimens were polished with 320, 600, and 1,000 SiC grit papers, degreased with acetone, rinsed with distilled water, and coated with paraffin wax so that only the gauge length was exposed to the test solutions. Tensile tests were carried out at room temperature (24±1 °C) in aerated (0.1 M, pH=4.74 and 0.5 M, pH=4.48) Na_2MoO_4 aqueous electrolytes at both open-circuit potential (OCP) and applied anodic potentials. The cell used was a 200-ml glass cylinder, closed by upper and lower stoppers, through which the ends of the specimen protruded. The failed specimens were cut 1 cm away from the fractured region and inspected by scanning electron microscopy (SEM). Electrochemical measurements were performed in (0.01 M, pH=4.93, 0.1 M, pH=4.74 and 0.5 M, pH=4.48) Na_2MoO_4 aqueous electrolytes on unstressed specimens. The potential was controlled using a Wenking Potentiostat L.T.73. The counter and reference electrodes were a platinum sheet and a saturated calomel electrode, respectively. The EFM data have been analyzed using Echem analyst 5.21. In this work, potential perturbation signal with amplitude of 10 mV with two sine waves of 2 and 5 Hz was applied. The intermodulation spectra containing current responses were assigned for harmonical and intermodulation current peaks. The larger peaks were used to calculate the corrosion current density (i_{corr}), the Tafel constants (β_c and β_a), and the causality factors CF-2 and CF-3.

Results and discussions

Stress corrosion cracking behavior

The engineering tensile stress (load per unit area) was recorded versus time for brass in different concentrations of molybdate solutions under OCPs as well as at different applied anodic potentials. A reference stress–time curve was made in air for comparison. Figure 1a, b shows the stress–time relations obtained for samples tested in 0.1 and 0.5 M Na_2MoO_4, respectively. It is clear that in both 0.1 and 0.5 M solutions under the OCP, the maximum stress before failure and the time to failure are less than the corresponding values obtained in air. Note that when the experiments were carried out under anodic polarization conditions, there was a further reduction in both maximum stress and time to failure. Figure 1c, d shows the corresponding stress–strain curves obtained under the same conditions as in Fig. 1a, b, respectively. The curves show the same conventional shape obtained for other alloys and are characterized by an increase in strain with increasing stress until the yield stress point is reached, followed by a slight gradual increase in the form of plateau until it reaches a maximum, after which the strain begins to decline to reach the point of failure [8]. The behavior obtained in air is also included for comparison and the results are summarized in Table 1.

The susceptibility (S) of the alloy to SCC was measured by the ratio of both the time to failure $\tau=t_f$ (solution)/t_f (air)

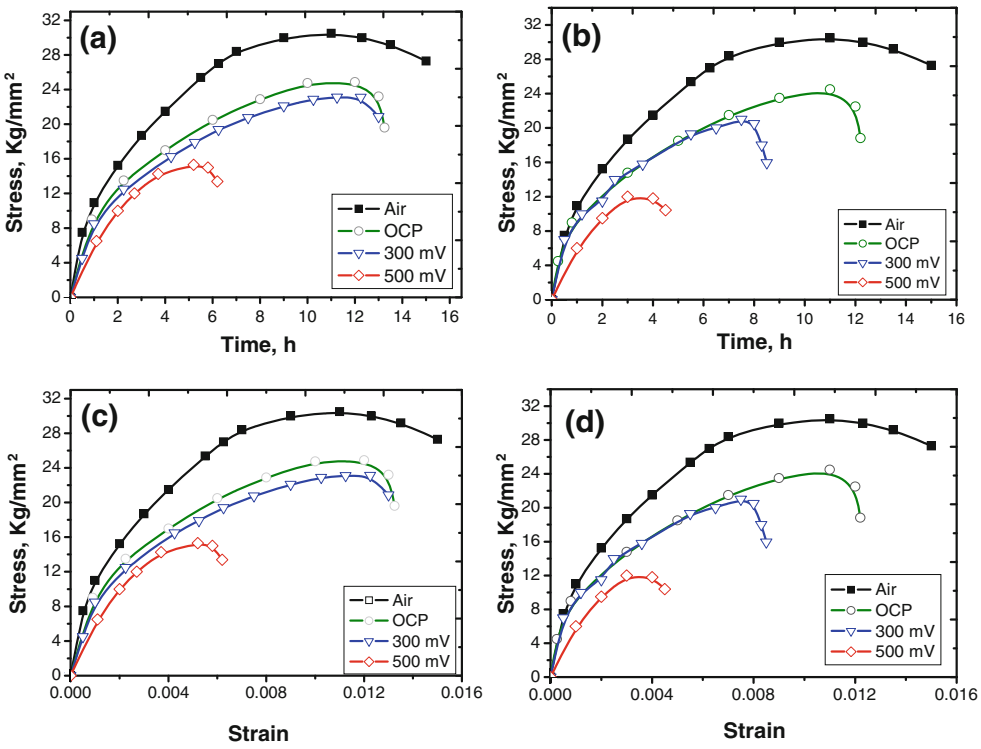

Fig. 1 **a**, **b** Stress–time and **c**, **d** stress–strain relations for specimens tested in 0.1 and 0.5 M Na_2MoO_4 electrolytes under a constant strain rate of 1.5×10^{-5} s^{-1}, respectively

and the maximum stress, the ratio of fracture stress in solution to that in air, $r=\sigma_{max}$ (solution)/σ_{max} (air). In general, as the ratio deviates from unity, the SCC severity increases. The authors previously showed that both r and τ can be combined in a quantitative expression for the susceptibility to SCC as follows [6]:

$$S = \sqrt{(1-r)(1-\tau)} \quad (1)$$

Examination of the data given in Table 1 reveals that SCC of brass is more severe under controlled anodic potentials than under OCP. It is also obvious that the severity of cracking increases with increasing the molybdate concentration. For example, under OCP, there is no susceptibility of brass towards SCC in 0.01 M molybdate solutions. However, the susceptibility increases by about 50% upon increasing the molybdate concentration from 0.1 to 0.5 M (S=0.117 to S=0.175). Note also that the time to failure at OCP decreases from 14 to 12 h upon increasing the molybdate concentration from 0.01 to 0.5 M. The application of anodic potentials shows a drastic effect on the deterioration of the material with the susceptibility found to increase in all cases as compared to those under OCP conditions. For example, the susceptibility towards

Table 1 SCC parameters of α-brass alloy in different concentrations of Na_2MoO_4 solutions at OCP and different anodic potentials

Concentration, M	E, mV_{NHE}	Time to failure, t_f (h/min)	Maximum stress ratio, r	τ	Susceptibility, S	Failure mode	Toughness, MJ m^{-3}
0.5	OCP	12:10	0.82	0.83	0.175	TC	292.80
	300	8:25	0.68	0.57	0.371	TC	171.28
	500	4:30	0.38	0.30	0.659	TC+IC	54.00
0.1	OCP	13:40	0.83	0.92	0.117	TC	328.93
	300	13:10	0.78	0.90	0.148	TC	299.13
	500	5:40	0.51	0.37	0.556	TC+IC	91.6
0.01	OCP	14:00	1.00	0.96	0	No C	–
	300	13:20	0.90	0.91	0.095	TC	–

TC transgranular SCC; *IC* intergranular SCC

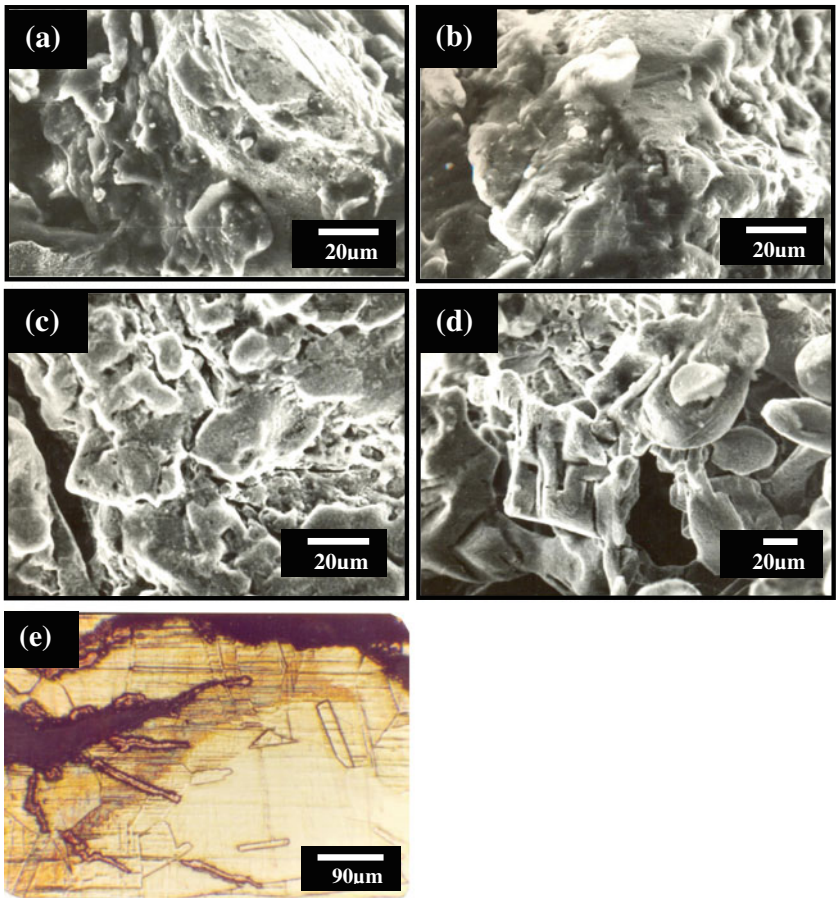

Fig. 2 SEM micrographs of specimens tested in 0.1 M Na_2MoO_4 solutions under a constant strain rate of 1.5×10^{-5} s^{-1} at **a** OCP, **b** 300 mV, **c**, **d** 500 mV of different magnifications. **e** Optical micrograph of the same specimen shown in **c**

SCC increases by ~280% for the specimen tested in 0.5 M when a potential of 500 mV was applied as compared to that tested under OCP (*S* increases from 0.175 to 0.659). Toughness, the area under the stress–strain curve, is also a useful criterion for assessing susceptibility to SCC [2]. Table 1 shows the obtained toughness values for specimens tested under OCP as well as under applied anodic potentials. Note that the toughness decreases from as high as 292.8 MJ/m^3 to only 54 MJ/m^3 for the specimen tested in 0.5 M Na_2MoO_4 solution at 500 mV as compared to that

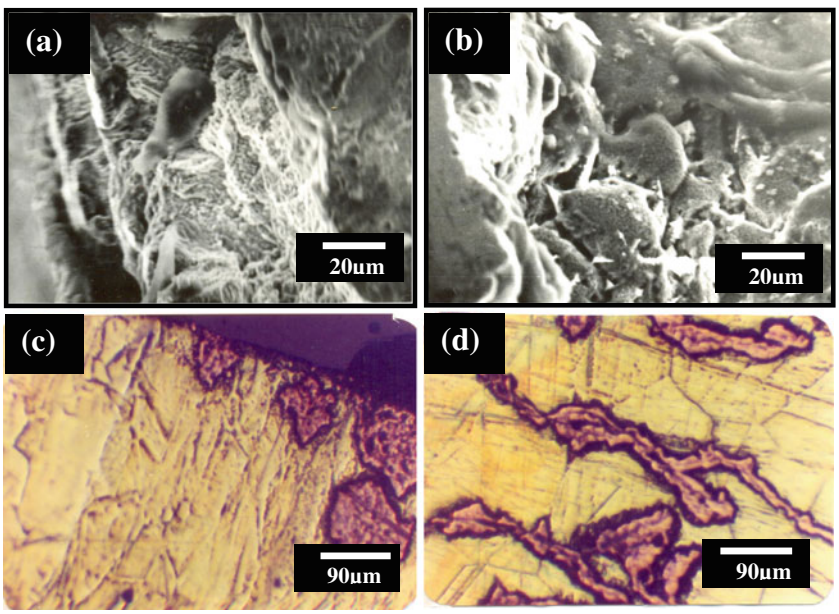

Fig. 3 **a**, **b** SEM micrographs of specimens tested in 0.5 M Na_2MoO_4 solutions under a constant strain rate of 1.5×10^{-5} s^{-1} at OCP and 300 mV, respectively. **c**, **d** Optical micrographs of specimens tested in 0.5 M Na_2MoO_4 solutions under a constant strain rate of 1.5×10^{-5} s^{-1} at 300 and 500 mV, respectively

tested at OCP in the same electrolyte. These results were further investigated by the fractographic inspection.

The fracture appearance of the failed specimens as revealed from SEM examination was the primary criterion for detecting the occurrence of SCC. Figures 2a and 3a show examples of SEM micrographs obtained for specimens failed at OCP in 0.1 and 0.5 M Na_2MoO_4 solutions, respectively. The cracking is entirely transgranular associated with pitting and dezincification. At moderately applied anodic potentials (300 mV), the mode of cracking is almost transgranular with some traces of intergranular cracking, see Figs. 2b and 3b. Note that the cracking is also associated with dezincification, see micrograph c of Fig. 3. Polarization at higher anodic potential (e.g., 500 mV) causes a transition of the mode of failure from transgranular to mixed trans- and intergranular cracking (Fig. 2c, d) with the degree of dezincification becomes more severe, see Figs. 2e and 3d. The severity of cracking increases with increasing molybdate concentration and anodic polarization potential as evidenced from the several deep and branched secondary cracks obtained in the specimens that have failed at 500 mV. These secondary cracks are associated with severe dezincification at the internal sides of the cracks even at the deepest points of cracks with the most severe cracking and dezincification obtained in 0.5 M Na_2MoO_4 solution at 500 mV. These observations are in accordance with the results from the fracture stress ratios, see Table 1. It is worth mentioning that the use of 0.01 M Na_2MoO_4 solutions resulted in SCC of brass only under applied anodic potentials but not at OCP. However, at higher concentrations, transgranular cracking, pitting corrosion, and mild dezincification were observed at OCP. It is possible that pitting with the help of stress may create intense anodic sites and lead to transgranular fracture. Parkins has mentioned that if crack propagation occurs by dissolution at an essentially film-free crack tip, the maintenance of film-free conditions may depend not only upon the electrochemical conditions existing in a pit but also upon the rate at which bare metal is created at the crack tip by plastic strain [9]. These conditions, in addition to dezincification, may lead to the formation of an embrittled zone.

At high anodic potentials, the appearance of intergranular cracking mixed with transgranular may be explained by the help of the anodic polarization behavior as explained in the next section. Briefly, the high values of the observed limiting current densities at those applied potentials cannot be regarded as true passivation. Corrosion will, therefore, be intensified locally through the pores of the films. It is suggested that preferential dissolution and mainly dezincification may take place at the pits and through the pores in air-formed film which enlarges with time and may lead an embrittled zone to crack fairly readily under a tensile load as suggested by Forty [10]. The grain boundary is more active and dissolves at a much faster rate than the grain interior [11], i.e., the anodic sites are the grain boundaries while the grain interiors act as cathodic sites. Interfacial energy considerations suggest that grain boundaries of brass are zinc rich [12]. Thus, localized zinc dissolution takes place at the grain boundary. In the presence of stress, these zones will crack fairly readily. Pickering and Byrne have shown that preferential Zn dissolution took place more readily on stressed brass [13].

Electrochemical behavior

The potential of unstressed α-brass specimens was followed as function of time until the steady state was attained, see Fig. 4a. It can be seen, in the solutions tested (0.1 and 0.5 M), that the potential values shift slightly with time to more noble (positive) values and attain the steady

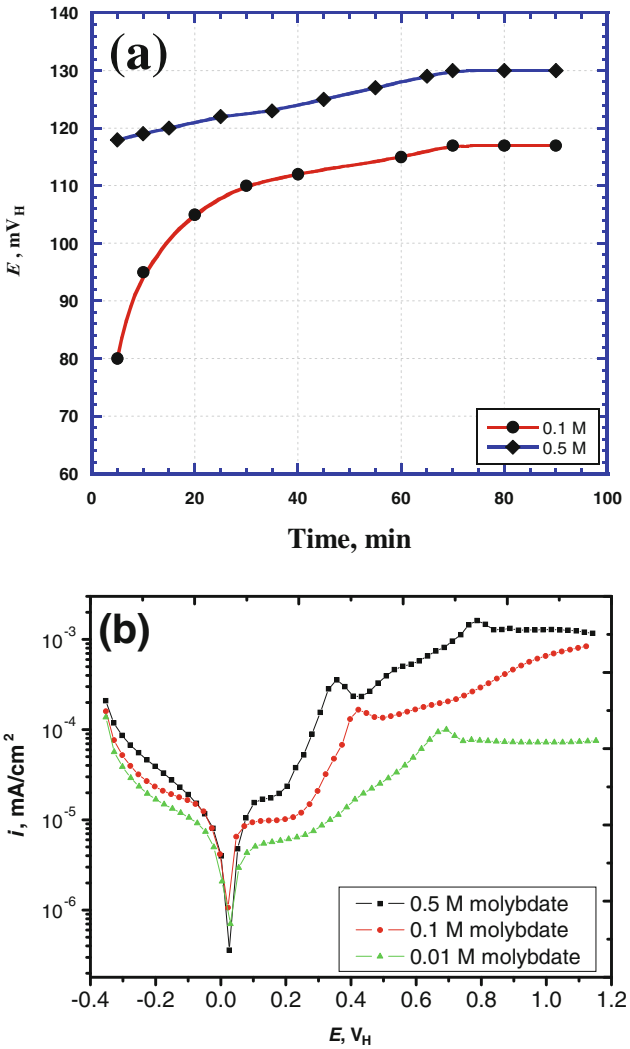

Fig. 4 **a** Potential–time curves and **b** potentiodynamic polarization curves of α-brass in Na_2MoO_4 solutions

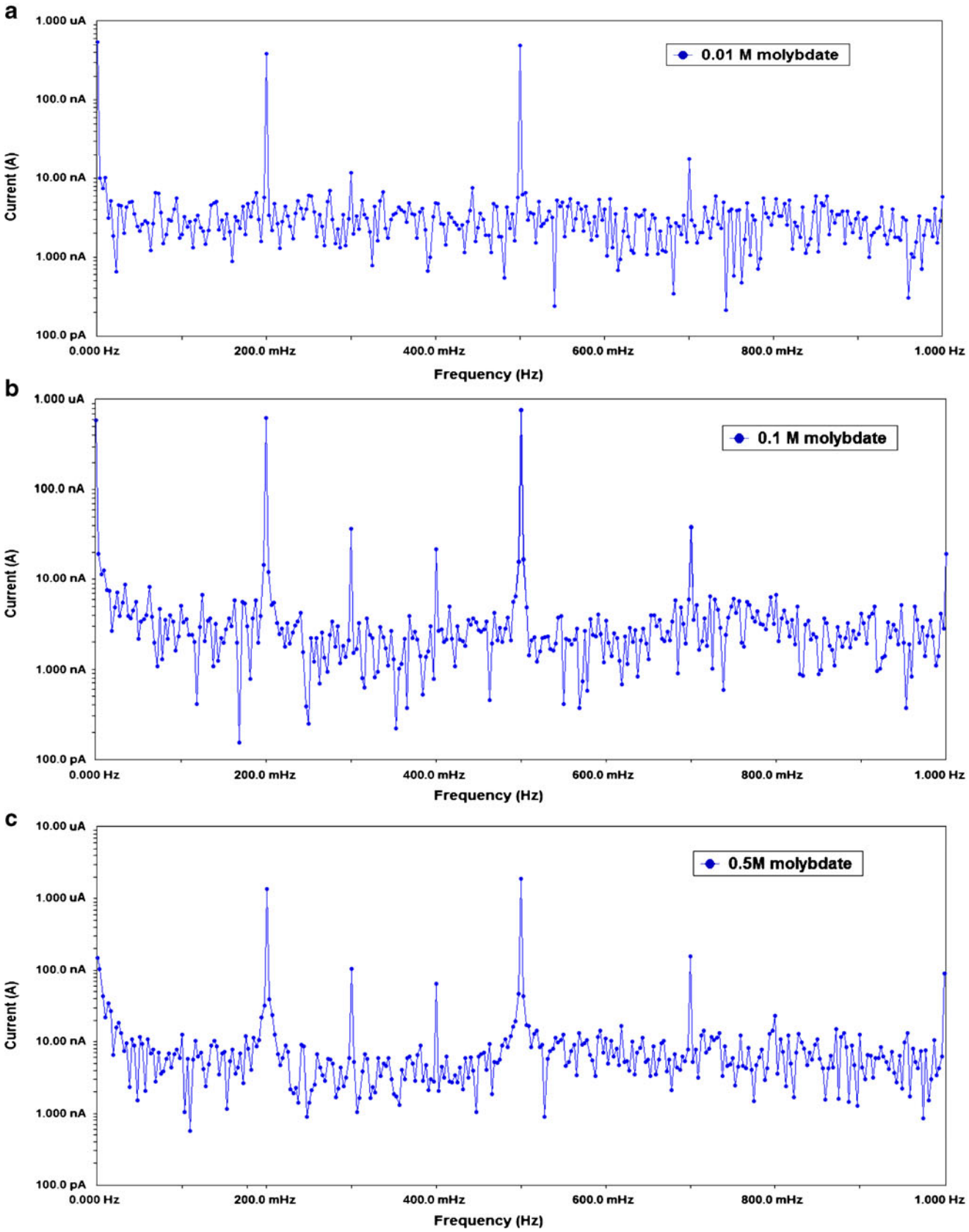

Fig. 5 Intermodulation spectra for α-brass in different concentrations of Na_2MoO_4. **a** 0.01 M, **b** 0.1 M, and **c** 0.5 M

state after ~60 min. On the other hand, the steady state potential in 0.5 M molybdate solution was more noble (by ~20 mV) as compared to that in 0.1 M solution.

The potentiodynamic polarization curves were also carried out for unstressed α-brass specimens in 0.5, 0.1, and 0.01 M Na_2MoO_4 solutions, see Fig. 4b. Note that the cathodic and anodic polarization curves are shifted to lower currents when the molybdate concentration decreases from 0.5 to 0.01 M. Also, the limiting current density decreases with decreasing the molybdate concentration from 0.5 to 0.1 M with a drastic decrease observed when the solution concentration was decreased down to 0.01 M. However, the corrosion potential (E_{corr}) is almost constant in the presence of the different concentrations of molybdate ions. Therefore, one can conclude that increasing the concentration of molybdate has caused a significant increase in the extent of corrosion attack on brass. Dezincification is considered the main cause of brass corrosion [14]. Upon dezincification, α-brass undergoes the following reaction:

$$Cu : Zn \rightarrow Cu + Zn^{2+} + 2e^{-} \quad (2)$$

After the outer surface of the brass is depleted of Zn and enriched in Cu, the brass undergoes simultaneous dissolution of Zn and Cu [15]. In our system, the presence of molybdate ions in the acidic media (pH≈4.5) can lead to the formation of partially soluble $ZnMoO_4$ [16]:

$$Zn^{2+} + MoO_4^{2-} \rightleftarrows ZnMoO_4 \quad (3)$$

Note that the possibility of hydrogen evolution may lead to the reduction of Mo^{6+} to Mo^{5+} which was indicated by the violet color [16] observed on the optical micrographs, see Figs. 2 and 3.

As corrosion process is a nonlinear electrochemical phenomenon, a potential perturbation signal by one or more sine waves is expected to generate current responses at more frequencies than those frequencies of the applied signal(s) [17]. In this regard, EFM measurements were performed to have a quantitative measure of the corrosion parameters. Briefly, EFM is a non-destructive corrosion measurement technique that can directly give values of corrosion current without prior knowledge of Tafel constants [17]. One more advantage of this technique is that the corrosion rate can be obtained instantaneously in very short time which makes this technique ideal in online corrosion monitoring. The results of EFM experiments are a spectrum of current response as a function of frequency. The spectrum is called the intermodulation spectrum and examples for the effect of addition of different concentrations of molybdate to α-brass alloy are shown in Fig. 5. The larger peaks with amplitudes of about 1 μA as the response to the 200 and 500 mHz excitation frequencies were used to calculate the corrosion current density (i_{corr}), the Tafel slopes (β_c and β_a), and the causality factors (CF-2 and CF-3). These electrochemical parameters were simultaneously determined and listed in Table 2. Note that the corrosion current density increases with increasing the concentration of molybdate ions with the corrosion rate of the alloy tested in 0.5 M molybdate solution (1.67 mils per year (mpy)) being at least four times higher than that measured in 0.01 M molybdate solution (0.4 mpy). The causality factors CF-2 and CF-3 are close to their expected theoretical values of 2 and 3, respectively, indicating the high accuracy of the measured data, i.e., there is a causal relationship between the perturbation signal and the response signal, and the measurements are not influenced by noise [18]. A commonly used parameter to monitor corrosion in industry is the polarization resistance (R_p) which can be related to the corrosion current by the Stern–Geary equation [19]:

$$i_{corr} = B/R_p \quad (4)$$

The proportionality constant, B, for a particular system can be calculated from β_a and β_c, the slopes of the anodic and cathodic Tafel lines. The relationship is given via:

$$B = \frac{\beta_a \beta_c}{2.3(\beta_a + \beta_c)}. \quad (5)$$

The calculated polarization resistance values from the EFM measurements are shown in Table 2. Note that R_p decreases with increasing molybdate ion concentration which is in line with the observed increase in corrosion rate. In general, the EFM results are in a good agreement with the data obtained from the potentiodynamic polarization technique indicating that the corrosion rate/current increases as the molybdate ion concentration increases.

Table 2 Electrochemical kinetic parameters obtained by EFM technique for α-brass in different concentrations of Na_2MoO_4 at 24±1 °C

Concentration, M	i_{corr}, μA cm^{-2}	β_a, mV decade^{-1}	$-\beta_c$, mV decade^{-1}	CF-2	CF-3	R_p, Ω cm^2	CR, mpy
0.01	0.88	113.6	148.0	1.92	2.88	31.75	0.40
0.10	1.62	120.7	201.7	1.84	2.81	20.27	0.74
0.50	3.65	107.6	231.9	1.76	2.78	8.75	1.67

CR corrosion rate

Conclusions

The electrochemical and stress corrosion cracking (SCC) behavior of 72Cu–28Zn alloy was studied in molybdate-containing electrolytes under OCP and anodic polarization. The use of 0.01 M Na_2MoO_4 solutions resulted in SCC of brass only under applied anodic potentials and not at OCP. However, at higher concentrations, transgranular cracking, pitting corrosion, and mild dezincification were observed even at OCP. SCC measurements and fractographic observations indicate that the susceptibility of the material tested in 0.5 M Na_2MoO_4 towards SCC increases by ~280% when a potential of 500 mV was applied as compared to that tested under OCP. The mode of failure was transgranular associated with pitting and dezincification at and near the open-circuit condition while the mode of failure became mixed trans- and intergranular associated with severe dezincification by anodic polarization.

The EFM measurements showed that the corrosion current density increases with increasing the concentration of molybdate ions with the corrosion rate of the alloy tested in 0.5 M molybdate solution being at least four times higher than that measured in 0.01 M molybdate solution under the same polarization conditions. These results are in agreement with the potentiodynamic measurements which showed that the limiting current density decreases with decreasing the molybdate concentration from 0.5 to 0.1 M with a drastic decrease observed when the solution concentration was decreased down to 0.01 M.

References

1. Davis JR (2001) Copper and copper alloys. ASM International, Materials Park
2. Allam NK, Ashour EA (2009) Mater Sci Eng B 156:84–89
3. Allam NK, Abdel Nazeer A, Ashour EA (2009) J Appl Electrochem 39:961–969
4. Kawashima A, Agraval AK, Staehle RW (1979) Stress corrosion cracking. In: Ugiansky GM, Payer AJ (eds) The slow strain rate technique. ASTM, Philadelphia
5. Kawashima A, Agraval AK, Staehle RW (1977) J Electrochem Soc 124:1822–1823
6. Allam NK, Abdel Nazeer A, Ashour EA (2010) Ind Eng Chem Res 49:9529–9533
7. Melendres CA, Hahn F, Bowmaker GA (2000) Electrochim Acta 46:9–13
8. Jones RH (1992) Stress corrosion cracking. ASTM International, Materials Park
9. Parkins RN, Holroyd NJH (1982) Corrosion 38:245–255
10. Forty AJ (1959) Physical metallurgy of stress corrosion fracture. Interscience, New York
11. Sircar SC, Chatterjee UK, Zamin M, Vijayendra HG (1972) Corros Sci 12:217–225
12. Speiser R, Spretnak JW (1956) Stress corrosion cracking and embrittlement. Wiley, New York
13. Pickering HW, Byrne PJ (1973) Corrosion 29:325–328
14. Kaiser H (1987) In: Mansfield F (ed) Alloys dissolution in corrosion mechanisms. Marcel Dekker, New York
15. Pickering HW (1983) Corros Sci 23:1107–1109
16. Koleske JV (1995) Paint and coating testing manual. ASTM, Philadelphia
17. Baboian R (2005) Corrosion tests and standards: application and interpretation, 2nd edn. ASTM International, Baltimore
18. Gamry Echem (2003) Analyst manual
19. Allam NK (2007) Appl Surf Sci 253:4570–4577